

Nonisothermal crystallization behavior and molecular dynamics of poly(lactic acid) plasticized with jojoba oil

Gamal R. Saad¹ · Moataz A. Elsayy² · Mohamed S. Abdel Aziz¹

Received: 29 June 2016 / Accepted: 13 October 2016 / Published online: 27 October 2016
© Akadémiai Kiadó, Budapest, Hungary 2016

Abstract Poly(lactic acid) (PLA) containing different contents of jojoba oil (3 and 7 mass%; namely PLA-3JO and PLA-7JO), as natural plasticizer, was prepared via melt compounding. The nonisothermal crystallization behavior of PLA in the presence of jojoba oil was investigated from the glassy state. The obtained results revealed that the rate of crystallization and degree of crystallinity increased with increasing the content of jojoba. The nonisothermal crystallization kinetics was analyzed by the Avrami–Jeziorny model. Avrami exponent (n) of the PLA, PLA-3JO and PLA-7JO was found to be 4.08, 3.28 and 3.09, respectively, suggesting that the nonisothermal cold crystallizations of the plasticized PLA follow a heterogeneous nucleation and three-dimensional spherulitic growth, as occurring in the neat PLA. Furthermore, the activation energy of nonisothermal crystallization process (ΔE_a) was calculated as a function of blend composition based on the Kissinger equation. It was found that the ΔE_a of PLA insignificantly changed in the presence of jojoba oil. The dielectric properties of totally amorphous and crystallized plasticized PLA were also investigated for the α -relaxation process as a function of the temperature and frequency. The α -relaxation process was analyzed with Havriliak–Negami and

Vogel–Fulcher–Tammann models, and fitting parameters with their evolution were discussed.

Keywords Poly(lactic acid) · Jojoba oil · Plasticization · Nonisothermal cold crystallization · Dielectric properties

Introduction

Poly(lactic acid) (PLA) is a linear, semicrystalline and biodegradable aliphatic polyester that can be produced from lactic acid by fermentation of renewable resources [1–3] and used as ecofriendly material [4–6]. PLA has good mechanical properties such as high mechanical strength, thermoplasticity and processability. However, PLA has some drawbacks that limit its wide application as a technical material, namely a relatively low impact resistance and low crystallization rate [7]. Thus, several modifications have been proposed to overcome these drawbacks, which include plasticization of PLA. The use of natural and/or biodegradable plasticizers, which are characterized by low toxicity, good compatibility and low migration, with biodegradable polymers, has attracted a lot of attention [8–12]. Compatibility between polymer and plasticizer is an important factor in choosing the external plasticizer, in order to produce a homogeneous and stable composition with reduced tendency for plasticizer migration [13, 14]. In a previous study, Moataz et al. used jojoba oil as a green plasticizer for PLA. They demonstrated that the elongation at a break point and Izod impact strength improve from 3.0 to 74 % and 12.9 ± 0.7 to 23.8 ± 1.6 kJ m⁻² with the addition of 7 mass% jojoba oil respectively, resulting in a toughened PLA [15].

Generally, it is well accepted that the mechanical and physical properties of the semicrystalline polymers are

Electronic supplementary material The online version of this article (doi:10.1007/s10973-016-5910-z) contains supplementary material, which is available to authorized users.

✉ Gamal R. Saad
grsaad@yahoo.com; grsaad@sci.cu.edu.eg

¹ Department of Chemistry, Faculty of Science, Cairo University, Giza 12613, Egypt

² Polymer Laboratory, Petrochemical Department, Egyptian Petroleum Research Institute, Nasser City, Cairo 11727, Egypt

governed by the morphology and supermolecular structure, which in turn is dominated by crystallization temperature and whether crystallization is performed from melt or from glassy state (histories). The crystallization behavior of neat PLA is extensively studied, especially the crystallization kinetics [16–19]; the isothermal melting mechanism [20–22]; the dimension of the crystal growth [16–22]; the effects of annealing on the thermal properties, morphology and mechanical properties of PLA films [23]; and the effects of thermal treatment on compression-molded PLA [24, 25].

In order to increase the crystallization rate three routes can be considered. The first one is to add a nucleating agent that will lower the surface free energy barrier toward nucleation and thus initiates crystallization at higher temperature upon cooling. A second possibility is to add a plasticizer which will increase the polymer chain mobility and will enhance the crystallization rate by reducing the energy required during crystallization for the chain folding process. The third possibility is to play with the molding conditions, in particular molding temperature and cooling time. The incorporation of plasticizer or/and nucleating agent [8, 26–30] into PLA matrix significantly change its crystallization behavior and therefore alter its physical and mechanical properties. In order to describe the macroscopic evolution of crystallinity under both isothermal and nonisothermal conditions (during the primary crystallization process), a number of mathematical models have been proposed [31–37]; among them, the so-called Avrami model is commonly used to analyze crystallization kinetics [33, 34]. It was reported that the PLA had a three-phase structure made of crystalline phase and two amorphous fractions [38–41]. In addition to the mobile amorphous fraction made of polymer chains that mobilize at the glass transition, a second fraction, the so-called rigid amorphous fraction, is the result of strong restrictions of amorphous chain segment mobility. The absolute value of the rigid amorphous fraction depends on whether it is formed during melt or cold crystallization and it was found to be around 10–35 % of the overall sample mass [41, 42]. Dielectric technique has widely been applied to monitor the kinetics of both cold and melt crystallization of semicrystalline polymers, including PLA [43–49]. In fact, the technique is particularly sensitive to the changes in the mobility of the different phases during the chain reorganization at the earlier stages.

This work aims to investigate the influence of the jojoba oil, as natural plasticizer, on the nonisothermal cold crystallization behavior of PLA. The molecular dynamics of the plasticized PLA was investigated by dielectric technique.

Experimental

Materials

The commercially available injection grade linear PLA, Ingeo™ 3001D, was supplied in pellet form by NatureWorks® LLC (Minnetonka, USA). The PLA has a density of 1.24 g cm^{-3} and a melt flow index of 15 dg min^{-1} ($190 \text{ }^\circ\text{C}/2.16 \text{ kg}$). The jojoba oil, a commercial grade, was purchased from Egyptian Natural Oil Company NATOIL (Cairo, Egypt).

Sample preparation

The neat PLA and jojoba oil were predried in vacuum oven at $80 \text{ }^\circ\text{C}$ for 24 h before use. PLA and jojoba oil were mixed together with different weight ratios of 100/0, 97/3 and 93/7 in a Prism Eurolab 16 co-rotating twin-screw extruder (Thermo Scientific). PLA containing 3.0 and 7.0 mass% jojoba oil are denoted here as PLA-3JO and PLA-7JO, respectively.

Measurements

Thermal behavior and crystallization kinetics of the neat PLA and PLA/JO blends were performed using a differential scanning calorimeter (DSC Q20, TA instrument, USA) under purge of nitrogen (50 mL min^{-1}). Temperature calibration was carried out using an indium standard. The sample weight was about 8–10 mg, and a new sample was used for each measurement to avoid degradation during the thermal analysis. For each measurement, sample of about 8.0 mg was placed in aluminum pan and heated to $190 \text{ }^\circ\text{C}$, where it was held for 3.0 min to erase the thermal history, and then rapidly cooled to $20 \text{ }^\circ\text{C}$ with cooling rate of $40 \text{ }^\circ\text{C min}^{-1}$. This allowed to obtain DSC curves of amorphous glassy material for different heating ramps. No remarkable exothermic event except the glass transition for all the investigated samples can be observed during the cooling process at the cooling rate of $40 \text{ }^\circ\text{C min}^{-1}$. This indicates that the neat PLA and plasticized PLA are not able to melt crystallized under such cooling condition even at a cooling rate $20 \text{ }^\circ\text{C min}^{-1}$ (see Supplemental information). For nonisothermal crystallization, the glassy amorphous samples were heated from 20 to $190 \text{ }^\circ\text{C}$ at different heating rates ($5, 10, 15$ and $20 \text{ }^\circ\text{C min}^{-1}$), and the glass transition temperature (T_g), the cold crystallization temperature (T_p) and the melting temperature (T_m) as well as the melting (ΔH_m) and the crystallization enthalpies (ΔH_{cc}) were determined.

Dielectric measurements were performed on Polymer Laboratories Dielectric Thermal Analyzer (PLDETA),

which gives directly the dielectric constant, ϵ' , and dielectric loss, ϵ'' . Dielectric measurements of wholly amorphous (first run) and crystallized samples (second run) were undertaken in temperature range from 20 to 150 °C at frequency range 0.2–100 kHz with a heating rate of 1.0 °C min⁻¹. Amorphous samples were obtained by rapid cooling of the molten polymer layers between stainless steel electrodes (30 mm in diameter), kept at 190 °C for 3 min, to a room temperature. Semicrystalline samples were obtained by heating the amorphous samples from 25 to 140 °C at heating rate 1.0 °C min⁻¹ and then annealed at 90 ± 1.0 °C for 2.0 h to attain equilibrium crystallinity. For frequency scan sweep of the amorphous samples, the frequency values were chosen within the range from 300 Hz to 100 kHz, in such a way that each spectrum was collected in a time that does not exceed 90 s to avoid the significant change in the crystallinity during the measurements. For all measurements, an appropriate Teflon spacer was used to control the sample thickness of 0.10–0.12 mm.

Results and discussion

Nonisothermal crystallization behavior

Figure 1 a, c shows the DSC thermographs of neat PLA and plasticized PLA with 3 and 7 mass% jojoba oil at different heating rates. The glass transition temperature (T_g), the cold crystallization (T_p) and the melting temperatures (T_m) are clearly seen. These values as well as the cold crystallization enthalpy (ΔH_{cc}) and melting enthalpy (ΔH_m) at different heating rates are summarized in Table 1. Also listed in this table the degree of crystallinity (χ_c %) of these samples calculated using the following equation:

$$X_c \% = 100 \times \frac{\Delta H_m}{w \cdot \Delta H_m^0} \quad (1)$$

where w is weight fraction of PLA and ΔH_m^0 is the enthalpy of fusion of 100 % crystalline PLA, and it has a value of 93 J g⁻¹ [24]. As shown from Table 1, the plasticized PLA shows a single glass transition, slightly lower than that of neat PLA, which was found to decrease with increasing plasticizer content. As it is expected, the peak cold crystallization shifts to higher temperature as a heating rate increases, meaning that the higher the heating rate the higher the temperature that the crystallization process started and completed. The addition of plasticizer significantly promoted recrystallization behavior of the PLA. This is a typical behavior of the plasticized thermoplastics, where the plasticizers promote the crystallinity due to the increase in the chain mobility. The higher plasticizer concentration shifted the crystallization peak to a lower temperature. This can be associated with two different

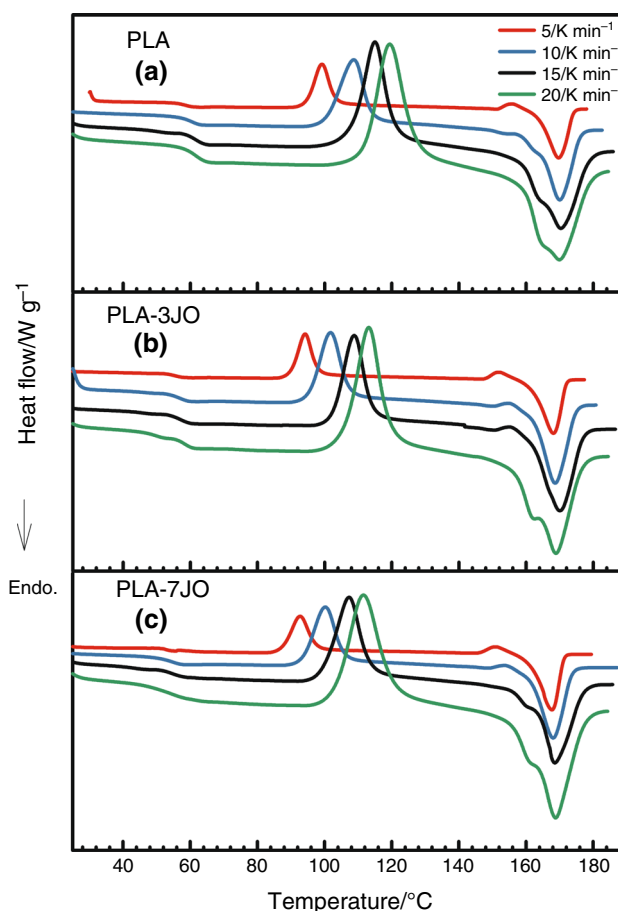


Fig. 1 DSC curves for the neat and plasticized PLA at different heating rates following a rapid cooling after being heated to 190 °C

phenomena. The first one is the increased chain mobility at low temperature associated with the depression of the T_g . This T_g reduction enables crystallization to start at a lower temperature upon heating. A second phenomenon is the reduced crystallization induction period due to the presence of crystalline nuclei already formed during the cooling process. A double melting is observed for neat and plasticized PLA. The peak at the lower temperature faded while the peak at the higher temperature became dominant with decreasing the heating rate. Such a double-melting behavior has also been observed by other authors for PLA systems [50–52] and reflects the melting process of crystals having different degrees of perfection; the lower- and higher-melting peaks may be corresponded to the melting of less and more perfect crystallites, respectively. The melting temperature of PLA does not significantly change in the presence of the plasticizer. A comparison between the enthalpy of crystallization and the melting enthalpy indicated that the enthalpy of crystallization is lower than that of melting. A more careful observation of the thermograms reveals the presence of a small exothermic peak prior to the major melting peak, especially at lower heating

Table 1 Thermal characteristics of the samples evaluated as determined by DSC

Sample code	$\phi/^\circ\text{C min}^{-1}$	$T_g/^\circ\text{C}$	$T_p/^\circ\text{C}$	$\Delta H_{cc}/\text{J g}^{-1}$	$T_m/^\circ\text{C}$	$\Delta H_m/\text{J g}^{-1}$	$\chi_c/\%$
PLA	5	58.8	99.2	31.3	169.6	39.2	42.2
	10	61.5	108.7	32.6	170.0	38.8	41.7
	15	61.6	115.0	32.3	170.3	37.9	40.8
	20	59.8	119.4	30.2	169.9	36.5	39.2
PLA-3JO	5	56.8	94.2	36.8	168.1	40.3	44.7
	10	57.1	102.7	30.0	168.7	40.8	44.2
	15	57.5	108.8	33.4	169.1	38.9	43.1
	20	58.3	113.2	37.5	168.9	39.7	44.0
PLA-7JO	5	53.8	92.7	35.1	167.7	38.6	44.6
	10	54.5	100.3	34.5	168.1	39.7	45.9
	15	54.5	107.3	33.4	168.6	39.3	45.4
	20	54.4	111.6	36.0	168.8	40.5	46.8

rate 5°C min^{-1} , which is characteristic of the α' phase of PLA [53], could be one explanation of this difference.

Nonisothermal crystallization kinetics

From the DSC curves, the relative crystallinity (X_T) as a function of temperature can be calculated from:

$$X_T = \frac{\int_{T_0}^T (dH_{cc}/dT) dT}{\Delta H_{cc}} \quad (2)$$

where T_0 and T represent the onset and an arbitrary temperature, respectively, and dH_{cc} is the enthalpy of cold crystallization released during an infinitesimal temperature range dT , and ΔH_{cc} is the overall enthalpy of cold crystallization for a specific heating condition.

Assuming that the sample experiences the same thermal history designated by the DSC furnace, the relation between crystallization time t and sample temperature T can be formulated as follows:

$$t = \frac{(T_0 - T)}{\phi} \quad (3)$$

where ϕ is the heating rate employed for the nonisothermal cold crystallization. The plots of the degree of crystallinity as a function of time X_t versus t for the neat and plasticized PLA cold crystallized nonisothermally at various heating rates are shown in Fig. 2. For each heating run, X_t increases exponentially with increasing crystallization time and finally levels off. The time taken to complete crystallization reduced with increasing heating rate, and the relative crystallinity of plasticized PLA was higher than that of neat PLA at a given time.

An important parameter which can be taken from the X_t curves is the half-time of cold crystallization $t_{1/2}$, which is the time interval from the onset of the cold crystallization

to the time at 50 % completion (Table 2). The obtained $t_{1/2}$ values decrease with increasing heating rate, indicating that the samples cold crystallize faster when the heating rate is increased. In addition, at the same heating rate, $t_{1/2}$ values of the plasticized PLA are lower than that of neat sample, confirming that the presence of jojoba oil enhances the crystallization process. The reciprocal value of $t_{1/2}$ (i.e., $1/t_{1/2}$ time $^{-1}$) signifies the cold crystallization rate. Comparison of the $1/t_{1/2}$ values for the neat and plasticized PLA, as given in Table 2, revealed that the cold crystallization rate of the neat PLA is lower than plasticized PLA and increased with increasing the jojoba oil content.

It is of great interest to evaluate the effect of jojoba oil on the crystallization rate of PLA in the plasticized samples quantitatively. A crystallization rate parameter (CRP), corresponding to the crystallization rate of polymers, was proposed by Zhang and co-workers [54, 55]. The CRP can be determined by the slope of a linear plot of $1/t_{1/2}$ versus heating rate, and a higher slope means a faster crystallization rate. Figure 3 shows the plots of $1/t_{1/2}$ versus heating rate for all the samples. The obtained CRP values are included in Table 2. The CRP values of the PLA loaded with jojoba oil are higher than that of neat one and increased with increasing content of jojoba oil, indicating that the rate of crystallization of PLA is promoted with incorporation of jojoba oil.

To quantitatively describe the nonisothermal crystallization kinetics, a number of models have been proposed in the literature [31–37, 56]. The most common approach is that based on the Avrami equation proposed by Jeziorny [34, 57]:

$$X_t = 1 - \exp(-K_t t^n) \quad (4)$$

where X_t is the relative degree of crystallinity, K_t is the crystallization rate constant depending on nucleation and growth rate, and n is the Avrami exponent depending on

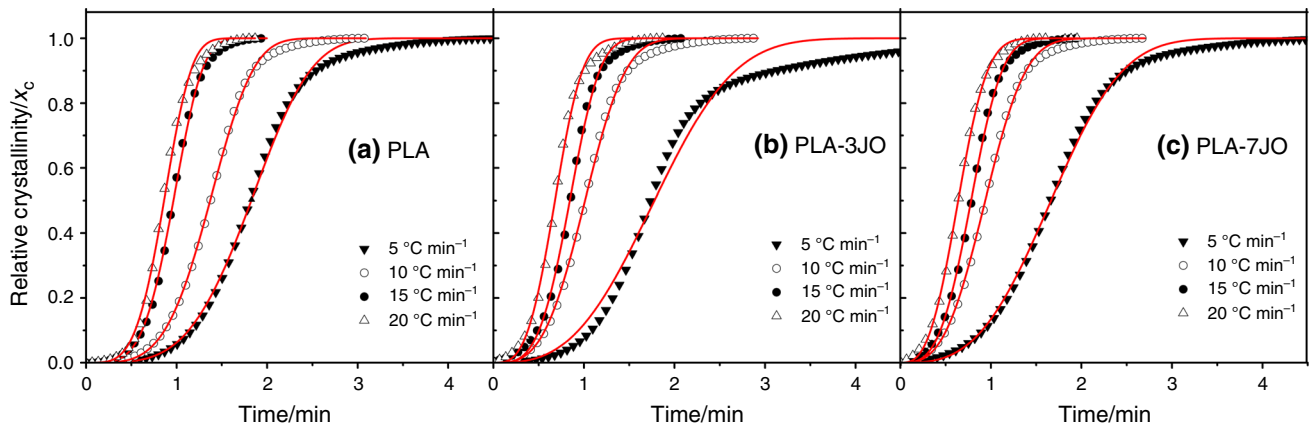


Fig. 2 Relative degree of crystallinity as a function of time at various heating rates for neat and plasticized PLA. The symbols represent experimental data while the continuous line represents the results of the theoretical Avrami model

Table 2 Nonisothermal crystallization parameters of neat and plasticized PLA

Sample code	$\phi/^\circ\text{C min}^{-1}$	$t_{1/2}/\text{min}$	$1/t_{1/2}/\text{min}^{-1}$	$\text{CRP}/^\circ\text{C}^{-1}$	n	K_t	K_c	r^2
PLA	5	1.815	0.551	4.4×10^{-2}	3.94	0.065	0.578	0.9982
	10	1.379	0.725		4.09	0.190	0.847	0.9994
	15	0.960	1.042		4.23	0.808	0.986	0.9991
	20	0.847	1.181		4.06	1.273	1.012	0.9981
PLA-3JO	5	1.737	0.576	5.7×10^{-2}	2.95	0.127	0.662	0.9880
	10	1.013	0.987		3.27	0.668	0.960	0.9986
	15	0.851	1.175		3.64	1.289	1.017	0.9981
	20	0.682	1.466		3.25	2.431	1.045	0.9975
PLA-7JO	5	1.660	0.602	6.2×10^{-2}	3.08	0.145	0.679	0.9984
	10	0.940	1.064		3.06	0.845	0.983	0.9990
	15	0.788	1.282		3.30	1.566	1.030	0.9991
	20	0.641	1.560		2.91	2.559	1.048	0.9994

the nature of nucleation and growth geometry of the crystals [33]. In order to estimate the Avrami parameters, K_t and n , a nonlinear curve-fitting procedure based on the Levenberg–Marquardt method was employed in this work using OriginPro 2016 software. The estimated values of K_t and n with those of the r^2 parameter are included in Table 2. Using these values for K_t and n , the relative crystallinity as a function of time can be calculated using Eq. (2). The theoretical lines thus produced are also plotted in Fig. 2 and compared to the experimental data. As it can be seen, the fit is well, meaning that the Avrami model is adequate to describe the nonisothermal crystallization kinetics of neat and plasticized PLA. Some minor deviations appear only for data that correspond to low (<5 %) or high (>90 %) relative degrees of crystallinity. At longer crystallization time, the deviation between the calculated trace from experimental data is probably due to the occurrence of impeded secondary crystallization that usually takes place in polymer crystallization at high

conversions. The K_t and n parameters do not have the same physical meaning as in the isothermal crystallization, because the temperature varies constantly in nonisothermal crystallization. This affects the rates of both nuclei formation and spherulite growth ascribed to their temperature dependence. Therefore, the crystallization rate constant K_t should be corrected adequately. Assuming a constant heating rate, the final form of crystallization rate constant can be corrected as suggested by Jeziorny [57] as follows:

$$\log K_c = \frac{\log K_t}{\phi} \quad (5)$$

It can be seen that the values of n for neat PLA were larger than that of plasticized PLA, which indicated that the addition of low molecular weight jojoba oil influences the mechanism of nucleation and the growth of PLA. The average n values of the PLA, PLA-3JO and PLA-7JO are 4.08, 3.28 and 3.09, respectively, suggesting that the non-isothermal cold crystallization of the plasticized PLA

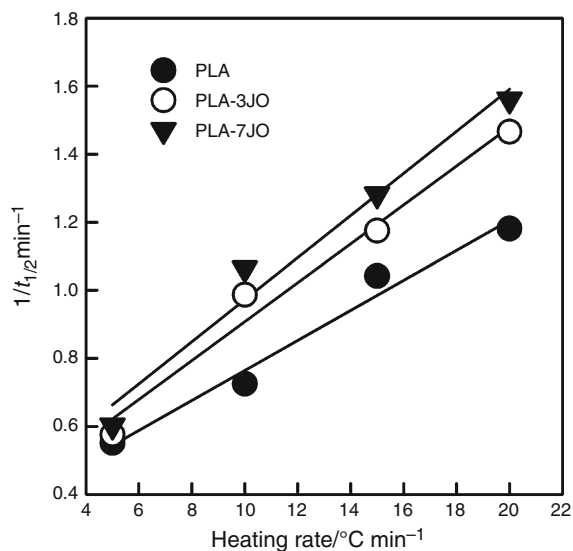


Fig. 3 Plots of reciprocal of $t_{1/2}$ as a function of heating rate for neat and plasticized PLA

follows a heterogeneous nucleation and three-dimensional spherulitic growth, as occurring in the neat PLA [58]. Similar to the case of $1/t_{1/2}$, the values of crystallization rate constant K_c are found to be dependent on the heating rate and the content of jojoba oil in the plasticized PLA samples. The K_c increased with increasing the heating rate and the content of jojoba oil at the same heating rate.

Activation energy of nonisothermal cold crystallization

The crystallization activation energy (E_a) is the activation energy required to transport molecular segments across the phase boundary to the crystallization surface [59]. It is an important parameter associated with nonisothermal cold crystallization. In a nonisothermal crystallization, the activation energy E_a can be derived from the variation of crystallization peak temperature T_p with heating rates by the Kissinger approach [60] as follows:

$$\frac{d \ln(\phi/T_p^2)}{d(1/T_p)} = -\frac{E_a}{R} \quad (6)$$

where ϕ is the heating rate, T_p is the cold crystallization peak temperature, and R is the universal gas constant. Plots of $\ln(\phi/T_p^2)$ versus $1/T_p$ of all samples are shown in Fig. 4, and they are fitted to straight lines. The E_a values calculated from the slopes are found to be 76.9 ± 1.1 , 77.8 ± 4.0 and 78.3 ± 5.6 kJ mol⁻¹ for PLA, PLA-3JO and PLA-7JO, respectively. The comparable E_a of neat and plasticized PLA suggested that presence of jojoba oil did

not significantly affect the energy required to transport molecular segments to the crystallization surface.

Dielectric relaxation of amorphous and crystallized samples

Figure 5 shows comparative isochronal plots of the dielectric constant (ϵ') and the dielectric loss (ϵ'') around glass transition temperatures of the amorphous (first run) and semicrystalline (second run) neat PLA and plasticized PLA at 100.0 kHz. The isochronal plots of dielectric constant (ϵ') and loss (ϵ'') at various frequencies of the wholly amorphous neat PLA and PLA-3JO, as a representative plasticized PLA sample, are represented in Figs. 6 and 7. For all amorphous samples, a gradual increase in the ϵ' is observed above 61 °C, which corresponds to the onset of the glass–rubber relaxation of the PLA matrix; this rise in ϵ' is accompanied by a narrow peak in ϵ'' corresponding to α -relaxation of the wholly amorphous phase of the PLA (denoted as α_{am}). At temperature above 83 °C, a sudden decrease in ϵ' is observed that reflects the onset of cold crystallization and this is followed by a faint second relaxation (denoted as α_{sc}) which assigned to the constrained segmental motions of the amorphous fraction confined between crystalline lamellae [43–48, 61, 62].

Comparison of the neat PLA with that of those of the plasticized PLA samples revealed that the increment of the ϵ' , associated with the glass–rubber transition, increases with increasing the content of jojoba oil and the drop in ϵ' due to crystallization starts at lower temperature. This may be attributed to increasing the segmental mobility of PLA

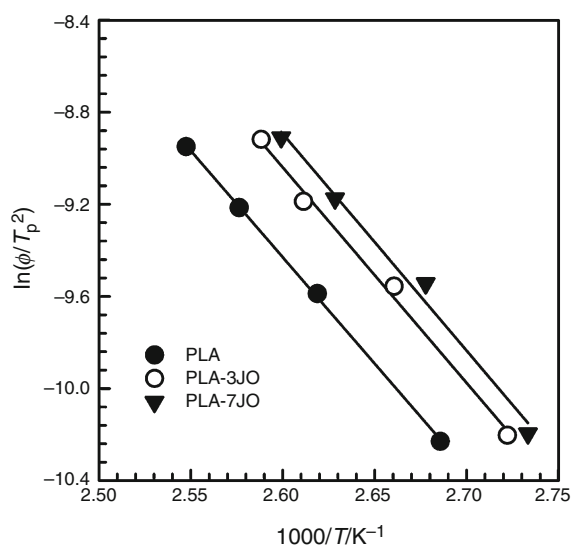
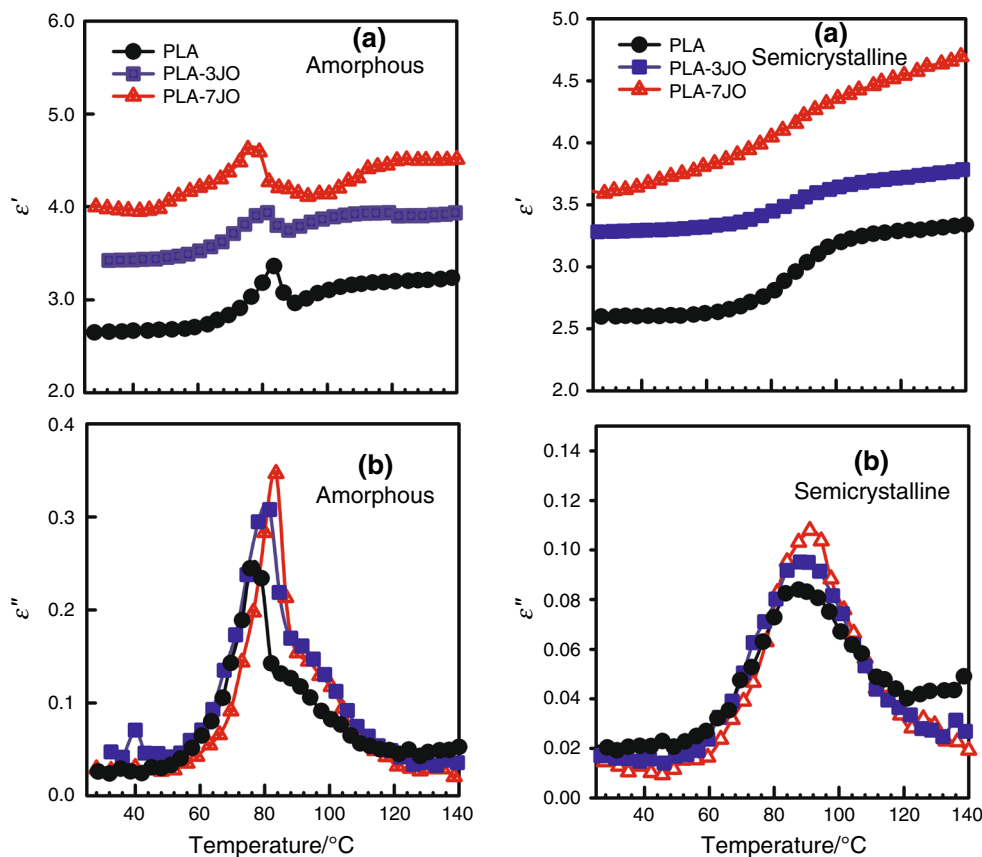


Fig. 4 Kissinger plots of the neat PLA and plasticized PLA cold crystallized nonisothermally with various heating rates

Fig. 5 Isochronal plots of **a** dielectric permittivity (ϵ') and **b** dielectric loss (ϵ'') of the amorphous and semicrystalline neat and plasticized PLA at 100 kHz



chains as a result of increasing their free volume due to loosened molecular packing of the PLA chains in the presence of jojoba. This observation is in agreement with the DSC data for the quenched samples that show enhanced cold crystallization of PLA in the presence of jojoba. Compared with the neat PLA, the loss peaks of the plasticized PLA, as the polymer chains experience much wider spectrum of segmental relaxation environments, exhibit a less intense and broaden. Both the α_{am} and α_{sc} -relaxation processes shifted toward higher temperatures when the frequency increased (Figs. 6 and 7). The observed increase in dielectric constant and loss above T_g , especially at lower frequencies and higher temperatures, might be related to the increase in ionic conductivity and/or electrode polarization [63].

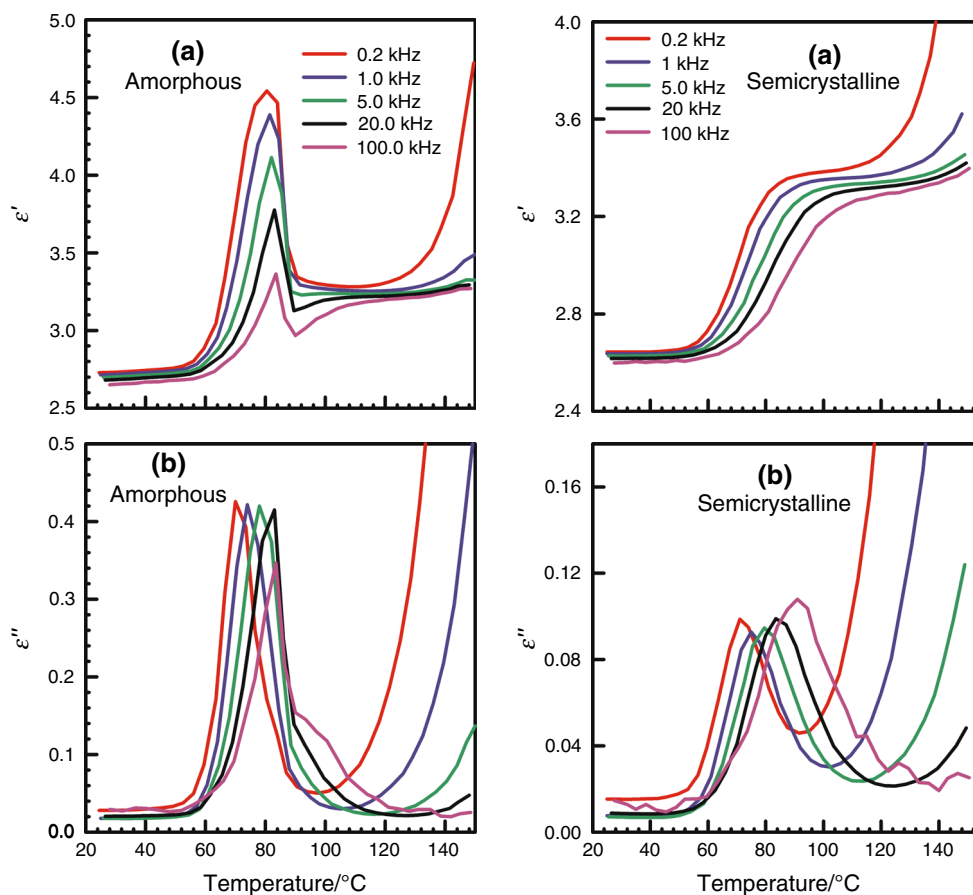
For nonisothermal crystallized samples (second scan), an increment in the ϵ' is observed around glass–rubber transition, which does not interfere with the effects of the cold crystallization during first scan. Additionally, the ϵ'' loss peaks became less intense and broadened due to the loss of dipoles that became immobilized as a result of the cold crystallization process and thus will not contribute to the dielectric response of the material. In contact to the amorphous, the loss peaks slightly shifted to higher

temperature with increasing jojoba oil. It is also remarkable that the position of the ϵ'' peak maximum for both the amorphous and crystallized shifted to lower temperature with increasing the content of the jojoba oil. Moreover, the intensity of ϵ' and the loss peaks decreased with increasing the jojoba oil content.

Dielectric analysis

Figure 8 shows frequency dependence of ϵ'' for totally amorphous and semicrystalline of the neat and plasticized PLA at 80 °C ($>T_g$). This temperature allows observing the α -relaxation process in the amorphous and crystallized samples. It can be clearly seen that both the loss peaks of the α_{am} and α_{sc} -relaxations of the PLA are amplified by the addition of jojoba. For the initially amorphous samples, the loss peak shifted to higher frequency (which means that the corresponding relaxation becomes faster) as the content of jojoba increase, probably due to the plasticization effect induced by the presence of jojoba oil. Regarding the crystallized samples, the loss peaks are less intense and broad, as expected for semicrystalline polymers [44–48, 64, 65], and their positions slightly shifted to higher temperature as the content of jojoba increase.

Fig. 6 Isochronal plots of **a** dielectric constant and **b** dielectric loss of amorphous and crystallized neat PLA at some selected frequencies



A more detailed analysis of the dielectric relaxation can be performed using the Havriliak–Negami (HN) equation [66]:

$$\varepsilon^* = \varepsilon_\infty + \frac{\Delta\varepsilon}{(1 + (i\omega\tau_0)^a)^b} \quad (7)$$

$$\Delta\varepsilon = \varepsilon_0 - \varepsilon_\infty \quad (8)$$

where ε_0 and ε_∞ are limiting low- and high-frequency dielectric constants, respectively, ω is the angular frequency, τ_0 is so-called Havriliak–Negami relaxation time and the exponents “ a ” and “ b ” are the shape parameters which characterize the width and the asymmetry of the loss curves. For the frequency-dependent conductivity contribution, conduction effects are treated in the usual way by adding contribution of $\sigma_0/\varepsilon_0\omega^s$ to the dielectric loss where σ_0 is related to the dc conductivity of the sample and ε_0 is the dielectric permittivity of vacuum (8.854×10^{-12} F m $^{-1}$). The parameter ($0 < s \leq 1.0$) describes for $s = 1$ Ohmic and for $s < 1.0$ non-Ohmic effects in the conductivity [67]. The shape of the α_{sc} -relaxation seems to be symmetric; the fitting parameter “ b ” was fixed at $b = 1.0$. In all preliminary fittings of the α_{am} -relaxation process of amorphous samples, the parameter b was always found to be around 0.55. In Fig. 8, the

lines going through the experimental points represent fitting result and the fitting parameters extracted from each relaxation are summarized in Table 3. It can be seen that the estimated symmetric shape parameter “ a ” for amorphous samples decreased from 0.79 to 0.59, while for the crystallized samples decreased from 0.49 to 0.41 with increasing the content of jojoba oil from 0.0 up to 7.0 %. This decrease is related to some changes in the morphological structure of PLA as a result of incorporation of jojoba oil, where the mobile amorphous and rigid amorphous fractions of PLA become more heterogeneous as the result of the presence of jojoba, and this in turn would give rise to different modes of segmental motions and, accordingly, to broad distribution relaxation times. The data listed in Table 3 demonstrated that the dielectric relaxation strength, $\Delta\varepsilon$, of the α_{am} and α_{sc} of the relaxation processes increased as the content of the jojoba oil increases, and this is also evident from the evolution of the peak height in the ε'' spectra for the raw data. Since the dielectric strength of the α -relaxation is characteristic of the mobile phase, the same interpretation is adopted for the increment of the dielectric strength in the plasticized samples as a result of plasticization. The fraction of the mobile amorphous segments (X_{maf}) in the crystallized samples that relax, at a given temperature, can be calculated by:

Fig. 7 Isochronal plots of **a** dielectric constant and **b** dielectric loss of amorphous and crystallized PLA-3JO at some selected frequencies

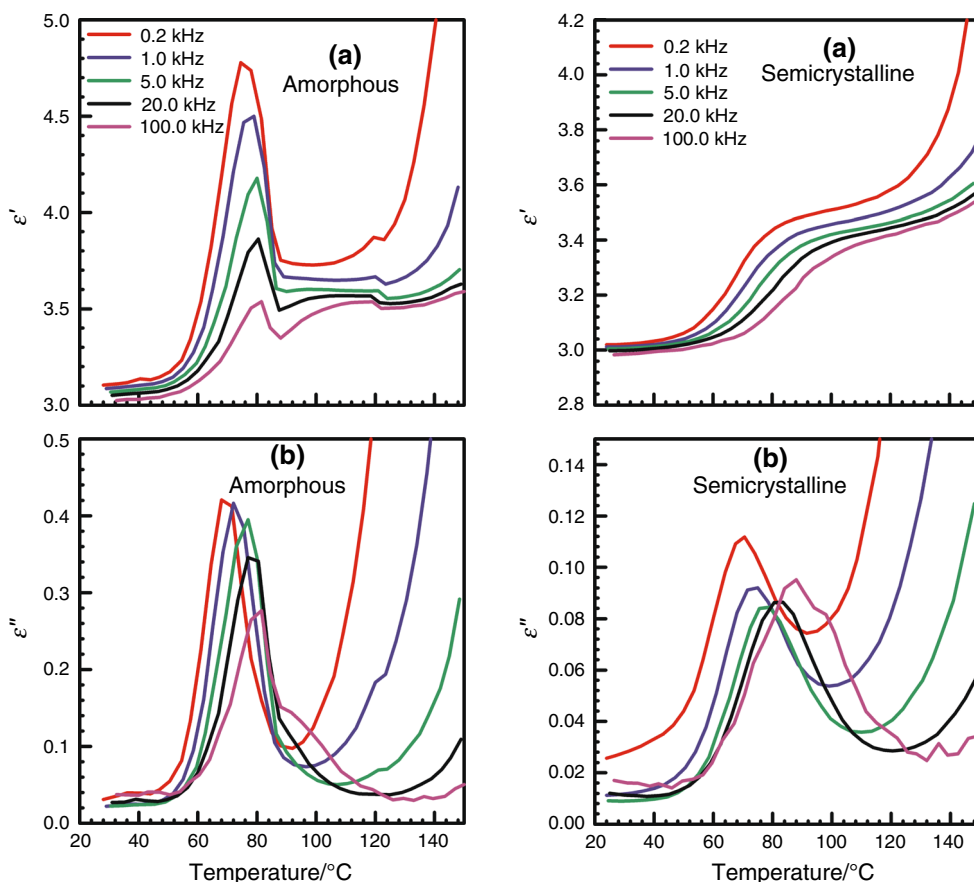
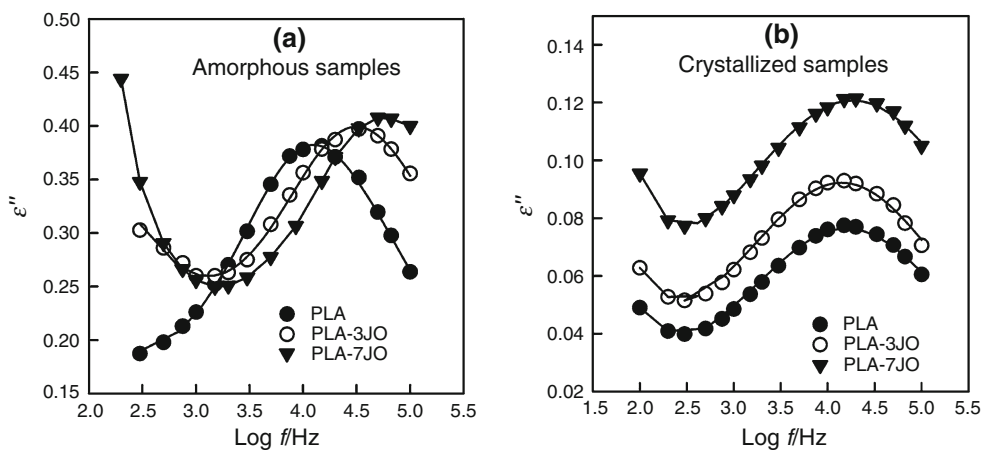


Fig. 8 Dielectric loss spectra of neat and plasticized PLA at 80 °C: **a** amorphous and **b** crystallized samples



$$X_{maf}(T) = \Delta\epsilon_{sc}(T)/\Delta\epsilon_{am}(T) \tag{9}$$

where $\Delta\epsilon_{sc}$ and $\Delta\epsilon_{am}$ are the relaxation strength of the crystallized and fully amorphous samples, respectively [62]. The values obtained are included in Table 3 and are used to calculate the rigid amorphous fraction (X_{raf}) based on a three-phase model, $X_{raf} = 1 - X_{maf} - X_c$, where X_c is the absolute crystalline fraction [calculated from DSC, Eq. (1)]. The X_{raf} value of the neat PLA is found to be 0.29, in a good agreement with the value reported by

Henricks et al. [42] using DSC technique. They demonstrated that the value of X_{raf} was 0.3 at the maximum crystallinity for the both cold- and melt-crystallized samples. As can be seen in Table 3, the X_{raf} values of PLA decreased with increasing the content of jojoba oil.

Typical temperature dependence of the relaxation time ($\tau = 1/2\pi f$) for α_{am} and α_{sc} -relaxation processes for the amorphous and crystallized samples is shown in Fig. 9; these data are taken from the isochronal dielectric loss curves (T_{max}) at different frequencies and can be described

Table 3 Dielectric fitting parameters at 80 °C and calculated rigid amorphous fraction of the neat and plasticized PLA crystallized isothermally at 80 °C

Parameters	Sample code		
	PLA	PLA-3JO	PLA-7JO
<i>Amorphous</i>			
$\Delta\epsilon$	1.18	1.37	2.01
a	0.79	0.75	0.59
τ	2.4×10^{-5}	9.0×10^{-6}	6.32×10^{-6}
B	1269	1226	1112
T_0	294	288	286
m	108	98	91
<i>Semicrystalline</i>			
$\Delta\epsilon$	0.36	0.44	0.70
a	0.52	0.50	0.42
τ	1.2×10^{-5}	1.10×10^{-5}	8.2×10^{-6}
B	1313	1345	1356
T_0	294	291	289
m	111	105	97
X_{raf}	0.29	0.24	0.20

by the Vogel–Fulcher–Tammann (VFT) relation [68–70], expressed by:

$$\tau = \tau_0 \exp\left(\frac{B}{T - T_0}\right) \quad (10)$$

where τ_0 is a pre-exponential factor, B is an activation parameter, and T_0 is a so-called Vogel temperature at which the main-chain motions are virtually frozen. The pre-exponential in Eq. (5) is sometimes identified with vibrational lifetimes [71], and thus a constant value of $\tau_0 = 1 \times 10^{-14}$ s was used for fitting data of all samples. The parameters extracted from the fit of these relaxation modes are included in Table 3. It is clear that the relaxation

time follows the VFT relation regardless of the presence and/or absence of crystalline phase and plasticizer. The obtained T_0 and B values of the amorphous neat PLA are 294 and 1269 K, respectively, in agreement with previous measurement [62]. A small increase in B value on going from amorphous to semicrystalline is observed, while T_0 remains the same. Regarding the changes in the VFT parameters for the amorphous and constrained segmental modes (α_{am} and α_{sc}) of the plasticized PLA, the results revealed that the B values decreased with increasing the content of the plasticizer. The T_0 of crystallized samples is higher than that of amorphous samples.

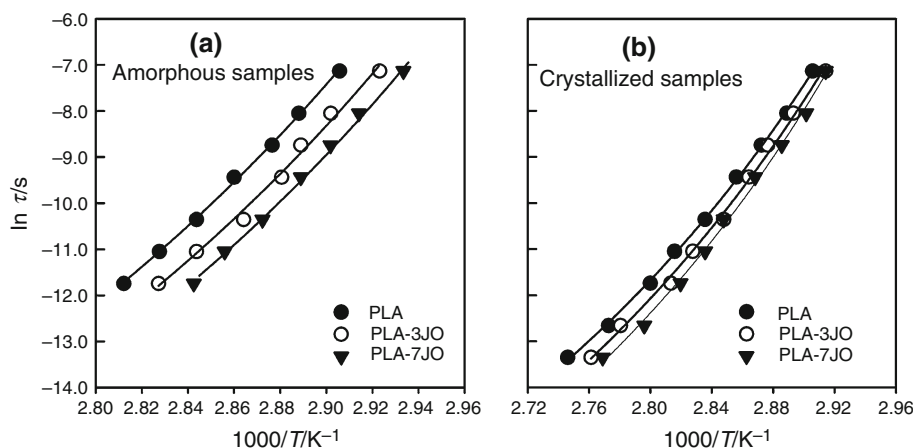
The dynamic fragility index, m , which describes the increase in the relaxation times as temperature comes closer to T_g is introduced by Angell [72]. Values of m are calculated by Eq. (6) using the VFT parameters (T_0 and B) are given in Table 3.

$$m = \left. \frac{d(\log \tau)}{d(T_{\text{ref}}/T_0)} \right|_{T=T_g} = \frac{BT_{\text{ref}}}{2.303(T_{\text{ref}} - T_0)^2} \quad (11)$$

where T_{ref} is a reference temperature when the segmental relaxation time (τ) is 100 s.

As shown in Table 3, the obtained m values are within the extreme values found in the fragility compilation made by Qin and McKenna on a variety of polymers [73] and comparable to the values reported previously for PLA and other bio-based polymers [74]. The m value obtained for neat and plasticized PLA can be considered as relatively fragile, which is by the way a classical behavior for macromolecules with Van der Waals or hydrogen bonds interactions between chains [72, 74]. Compared plasticized PLA with neat PLA revealed that the plasticized samples seem to be less fragile. A small decrement of the m values with increasing the content of jojoba is also observed. The decrease in these values may be attributed to an increase in the amorphous molecular mobility as the result of plasticization effect of jojoba oil.

Fig. 9 Temperature dependences of the relaxation times for the α_{am} and α_{sc} -relaxation processes for neat PLA and plasticized PLA, and solid lines are the VFT fit



Conclusions

The nonisothermal cold crystallization behavior PLA plasticized with jojoba was studied using differential scanning calorimetry. The results showed that the cold crystallization temperature (T_p) of the PLA decreased, while the melting peak did not significantly change with increasing the jojoba content. Avrami–Jeziorny model was applied to analyze the nonisothermal crystallization process; according to the obtained data, the Avrami exponent (n) indicated that both neat PLA and plasticized PLA follow a heterogeneous nucleation and three-dimensional spherulitic growth. Comparison of half-life crystallization times and the rate constant (K_c) revealed that the rate of crystallization of PLA increased with increasing the jojoba content. The incorporation of jojoba in PLA did not significantly change the kinetic energy of the crystallization.

The dielectric spectra of the amorphous plasticized PLA showed that two main α -relaxation one corresponding to the wholly amorphous phase (α_{am}) and the other, which appeared at relatively higher temperature, is assigned to the constrained amorphous phase (α_{sc}) between crystalline lamellae. The intensity of the ϵ'' maxima of both α_{am} and α_{sc} increased with increasing the content of jojoba oil and shifted to lower temperature as the result of plasticization effect of jojoba. The dielectric data were fitted reasonably well to the semiempirical HN equation. The broadness of the relaxation peaks and the dielectric strength of the both the amorphous and semicrystalline samples increased with increasing the content of jojoba. From the temperature dependence of the relaxation times of the α -processes, the Vogel–Fulcher–Tammann parameters were estimated. The structural relaxation analysis revealed a classical polymeric “fragile” behavior for neat and plasticized PLA, and the fragility index slightly decreased with increasing the jojoba. The difference may be associated with the increase in chains mobility, due to plasticization effect of jojoba.

References

- Chandra R, Rustgi R. Biodegradable polymers. *Prog Polym Sci*. 1998;23(7):1273–335.
- Warwel S, Brüse F, Demes C, Kunz M, gen Klaas MR. Polymers and surfactants on the basis of renewable resources. *Chemosphere*. 2001;3(1):39–48.
- Avérous L. Poly(lactic acid): synthesis, properties and applications. In: Belgacem MN, Gandini A, editors. *Monomers, polymers and composites from renewable resources*. Amsterdam: Elsevier; 2008. p. 433–50.
- Hausberger AG, DeLuca PP. Characterization of biodegradable poly(D,L-lactide-co-glycolide) polymers and microspheres. *J Pharm Biomed Anal*. 1995;13(6):747–60.
- Sinclair R. The case for polylactic acid as a commodity packaging plastic. *J Macromol Sci Part A Pure Appl Chem*. 1996;33(5):585–97.
- Okada M. Chemical syntheses of biodegradable polymers. *Prog Polym Sci*. 2002;27(1):87–133.
- Albertsson A-C, Varma IK. *Aliphatic polyesters: synthesis, properties and applications*. Degradable aliphatic polyesters. Berlin: Springer; 2002. p. 1–40.
- Baiardo M, Frisoni G, Scandola M, Rimelen M, Lips D, Ruffieux K, et al. Thermal and mechanical properties of plasticized poly(L-lactic acid). *J Appl Polym Sci*. 2003;90(7):1731–8.
- Kulinski Z, Piorkowska E. Crystallization, structure and properties of plasticized poly(L-lactide). *Polymer*. 2005;46(23):10290–300.
- Murariu M, Da Silva Ferreira A, Alexandre M, Dubois P. Poly(lactide (PLA) designed with desired end-use properties: 1. PLA compositions with low molecular weight ester-like plasticizers and related performances. *Polym Adv Technol*. 2008;19(6):636–46.
- Hassouna F, Raquez J-M, Addiego F, Dubois P, Toniazzi V, Ruch D. New approach on the development of plasticized poly(lactide (PLA): grafting of poly(ethylene glycol)(PEG) via reactive extrusion. *Eur Polym J*. 2011;47(11):2134–44.
- Vieira MGA, da Silva MA, dos Santos LO, Beppu MM. Natural-based plasticizers and biopolymer films: a review. *Eur Polym J*. 2011;47(3):254–63.
- Sears JK, Darby JR. *The technology of plasticizers*. New York: Wiley; 1982.
- Cakar F, Yazici O, Cankurtaran O, Karaman F. A study on compatibility of polymer blends of poly(2,6-dimethyl-1,4-phenyleneoxide)/poly(ether imide). *Optoelectron Adv Mater*. 2012;6:1153–6.
- Elsawy M, Christiansen JdC, Sanporean C-G. Investigation of jojoba oil-wax as a plasticizer for poly(lactic acid). *Optoelectron Adv Mater*. 2014;8(1–2):109–14.
- Kalb B, Pennings AJ. General crystallization behaviour of poly(L-lactic acid). *Polymer*. 1980;21(6):607–12.
- Urbanovici E, Schneider H, Brizzolaro D, Cantow H. Isothermal melt crystallization kinetics of poly(L-lactic acid). *J Therm Anal Calorim*. 1996;47(4):931–9.
- Tabi T, Sajó I, Szabó F, Luyt A, Kovács J. Crystalline structure of annealed polylactic acid and its relation to processing. *Express Polym Lett*. 2010;4(10):659–68.
- Badrinarayanan P, Dowdy KB, Kessler MR. A comparison of crystallization behavior for melt and cold crystallized poly(L-lactide) using rapid scanning rate calorimetry. *Polymer*. 2010;51(20):4611–8.
- Vasanthakumari R, Pennings A. Crystallization kinetics of poly(L-lactic acid). *Polymer*. 1983;24(2):175–8.
- Yasuniwa M, Tsubakihara S, Sugimoto Y, Nakafuku C. Thermal analysis of the double-melting behavior of poly(L-lactic acid). *J Polym Sci B Polym Phys*. 2004;42(1):25–32.
- Di Lorenzo ML. Calorimetric analysis of the multiple melting behavior of poly(L-lactic acid). *J Appl Polym Sci*. 2006;100(4):3145–51.
- Tsuji H, Ikada Y. Properties and morphologies of poly(L-lactide): 1. Annealing condition effects on properties and morphologies of poly(L-lactide). *Polymer*. 1995;36(14):2709–16.
- Migliaresi C, Cohn D, De Lollis A, Fambri L. Dynamic mechanical and calorimetric analysis of compression-molded PLLA of different molecular weights: effect of thermal treatments. *J Appl Polym Sci*. 1991;43(1):83–95.
- Pantani R, De Santis F, Sorrentino A, De Maio F, Titomanlio G. Crystallization kinetics of virgin and processed poly(lactic acid). *Polym Degrad Stab*. 2010;95(7):1148–59.
- Ljungberg N, Wesslén B. Preparation and properties of plasticized poly(lactic acid) films. *Biomacromolecules*. 2005;6(3):1789–96.

27. Ke T, Sun X. Melting behavior and crystallization kinetics of starch and poly(lactic acid) composites. *J Appl Polym Sci*. 2003;89(5):1203–10.
28. Gumus S, Ozkoc G, Aytac A. Plasticized and unplasticized PLA/ organoclay nanocomposites: Short-and long-term thermal properties, morphology, and nonisothermal crystallization behavior. *J Appl Polym Sci*. 2012;123(5):2837–48.
29. Battagazzore D, Bocchini S, Frache A. Crystallization kinetics of poly(lactic acid)-talc composites. *Express Polym Lett*. 2011;5(10):849–58.
30. Li H, Huneault MA. Effect of nucleation and plasticization on the crystallization of poly(lactic acid). *Polymer*. 2007;48(23):6855–66.
31. Kolmogorov AN. On the statistical theory of the crystallization of metals. *Bull Acad Sci USSR Math Ser*. 1937;1:355–9.
32. Johnson WA, Mehl RF. Reaction kinetics in processes of nucleation and growth. *Trans Aime*. 1939;135(8):396–415.
33. Avrami M. Kinetics of phase change. I General theory. *J Chem Phys*. 1939;7(12):1103–12.
34. Avrami M. Kinetics of phase change. II transformation–time relations for random distribution of nuclei. *J Chem Phys*. 1940;8(2):212–24.
35. Tobin MC. Theory of phase transition kinetics with growth site impingement. I. Homogeneous nucleation. *J Polym Sci Part B Polym Phys*. 1974;12(2):399–406.
36. Tobin MC. The theory of phase transition kinetics with growth site impingement. II. Heterogeneous nucleation. *J Polym Sci Part B Polym Phys*. 1976;14(12):2253–7.
37. Malkin AY, Beghishev V, Keapin IA, Bolgov S. General treatment of polymer crystallization kinetics—part 1. A new macrokinetic equation and its experimental verification. *Polym Eng Sci*. 1984;24(18):1396–401.
38. Saiter A, Delpouve N, Dargent E, Saiter J. Cooperative rearranging region size determination by temperature modulated DSC in semi-crystalline poly(L-lactide acid). *Eur Polym J*. 2007;43(11):4675–82.
39. Magoń A, Pyda M. Study of crystalline and amorphous phases of biodegradable poly(lactic acid) by advanced thermal analysis. *Polymer*. 2009;50(16):3967–73.
40. Di Lorenzo ML, Cocca M, Malinconico M. Crystal polymorphism of poly(L-lactic acid) and its influence on thermal properties. *Thermochim Acta*. 2011;522(1):110–7.
41. Delpouve N, Saiter A, Dargent E. Cooperativity length evolution during crystallization of poly(lactic acid). *Eur Polym J*. 2011;47(12):2414–23.
42. Henricks J, Boyum M, Zheng W. Crystallization kinetics and structure evolution of a polylactic acid during melt and cold crystallization. *J Therm Anal Calorim*. 2015;120(3):1765–74.
43. Kanchanasopa M, Runt J. Broadband dielectric investigation of amorphous and semicrystalline L-lactide/meso-lactide copolymers. *Macromolecules*. 2004;37(3):863–71.
44. Brás AR, Viciosa MT, Wang Y, Dionísio M, Mano JF. Crystallization of poly(L-lactic acid) probed with dielectric relaxation spectroscopy. *Macromolecules*. 2006;39(19):6513–20.
45. Wurm A, Soliman R, Schick C. Early stages of polymer crystallization—a dielectric study. *Polymer*. 2003;44(24):7467–76.
46. Ren J, Adachi K. Dielectric relaxation in blends of amorphous poly(DL-lactic acid) and semicrystalline poly(L-lactic acid). *Macromolecules*. 2003;36(14):5180–6.
47. Dionísio M, Viciosa MT, Wang Y, Mano JF. Glass transition dynamics of poly(L-lactic acid) during isothermal crystallisation monitored by real-time dielectric relaxation spectroscopy measurements. *Macromol Rapid Commun*. 2005;26(17):1423–7.
48. Bras A, Malik P, Dionísio M, Mano J. Influence of crystallinity in molecular motions of poly(L-lactic acid) investigated by dielectric relaxation spectroscopy. *Macromolecules*. 2008;41(17):6419–30.
49. Soccio M, Nogales A, Lotti N, Munari A, Ezquerria TA. The β relaxation as a probe to follow real-time polymer crystallization in model aliphatic polyesters. *Polymer*. 2007;48(16):4742–50.
50. Ling X, Spruiell JE. Analysis of the complex thermal behavior of poly(L-lactic acid) film. I. Samples crystallized from the glassy state. *J Polym Sci B Polym Phys*. 2006;44(22):3200–14.
51. Abe H, Harigaya M, Kikkawa Y, Tsuge T, Doi Y. Crystal growth and solid-state structure of poly(lactide) stereocopolymers. *Biomacromolecules*. 2005;6(1):457–67.
52. Pluta M, Jeszka J, Boiteux G. Polylactide/montmorillonite nanocomposites: structure, dielectric, viscoelastic and thermal properties. *Eur Polym J*. 2007;43(7):2819–35.
53. Zhang J, Tashiro K, Tsuji H, Domb AJ. Disorder-to-order phase transition and multiple melting behavior of poly(L-lactide) investigated by simultaneous measurements of WAXD and DSC. *Macromolecules*. 2008;41(4):1352–7.
54. Zhang R, Zheng H, Lou X, Ma D. Crystallization characteristics of polypropylene and low ethylene content polypropylene copolymer with and without nucleating agents. *J Appl Polym Sci*. 1994;51(1):51–6.
55. Wu M, Yang G, Wang M, Wang W, Zhang W-D, Feng J, et al. Nonisothermal crystallization kinetics of ZnO nanorod filled polyamide 11 composites. *Mater Chem Phys*. 2008;109(2):547–55.
56. Di Lorenzo M, Silvestre C. Non-isothermal crystallization of polymers. *Prog Polym Sci*. 1999;24(6):917–50.
57. Jeziorny A. Parameters characterizing the kinetics of the non-isothermal crystallization of poly(ethylene terephthalate) determined by DSC. *Polymer*. 1978;19(10):1142–4.
58. Schulz E, Wunderlich B. *Macromolecular physics, vol. 2 crystal nucleation, growth, annealing*. New York: Academic; 1976. p. 50.
59. Wu TM, Chen EC. Crystallization behavior of poly(ϵ -caprolactone)/multiwalled carbon nanotube composites. *J Polym Sci B Polym Phys*. 2006;44(3):598–606.
60. Kissinger HE. Variation of peak temperature with heating rate in differential thermal analysis. *J Res Natl Inst Stand Technol*. 1956;57(4):217–21.
61. Jeszka J, Pietrzak L, Pluta M, Boiteux G. Dielectric properties of polylactides and their nanocomposites with montmorillonite. *J Non-Cryst Solids*. 2010;356(11):818–21.
62. Laredo E, Grimau M, Bello A, Wu D. Molecular dynamics and crystallization precursors in polylactide and poly(lactide)/CNT biocomposites in the insulating state. *Eur Polym J*. 2013;49(12):4008–19.
63. McCrum NG, Read BE, Williams G. *Anelastic and dielectric effects in polymeric solids*. New York: Wiley; 1967.
64. Mijovic J, Sy J-W. Molecular dynamics during crystallization of poly(L-lactic acid) as studied by broad-band dielectric relaxation spectroscopy. *Macromolecules*. 2002;35(16):6370–6.
65. Kortaberria G, Marieta C, Jimeno A, Arruti P, Mondragon I. Crystallization of poly(L-lactid acid) monitored by dielectric relaxation spectroscopy and atomic force microscopy. *J Microsc*. 2006;224(3):277–89.
66. Havriliak S, Negami S. A complex plane representation of dielectric and mechanical relaxation processes in some polymers. *Polymer*. 1967;8:161–210.
67. Böttcher CJP, van Belle OC, Bordewijk P, Rip A. *Theory of electric polarization*. Amsterdam: Elsevier; 1978.
68. Tammann G, Hesse W. Die Abhängigkeit der Viskosität von der Temperatur bei unterkühlten Flüssigkeiten. *Z Anorg Allg Chem*. 1926;156(1):245–57.
69. Fulcher GS. Analysis of recent measurements of the viscosity of glasses. *J Am Ceram Soc*. 1925;8(6):339–55.
70. Vogel H. The law of the relation between the viscosity of liquids and the temperature. *Physikalische Zeitschrift*. 1921;22:645–6.

71. Jin X, Zhang S, Runt J. Dielectric studies of poly(ethylene oxide)/poly(styrene-co-*p*-hydroxystyrene) blends: influence of hydrogen bonding on the dynamics of amorphous blends. *Macromolecules*. 2003;36(21):8033–9.
72. Angell CA. In: Nagai KL, Wright CB, editors. *Relaxation in complex systems*. Washington, DC: NRL; 1985. p. 3–12.
73. Qin Q, McKenna GB. Correlation between dynamic fragility and glass transition temperature for different classes of glass forming liquids. *J Non-Cryst Solids*. 2006;352(28):2977–85.
74. Arnoult M, Dargent E, Mano J. Mobile amorphous phase fragility in semi-crystalline polymers: comparison of PET and PLLA. *Polymer*. 2007;48(4):1012–9.